Double hysteresis loops in 0.91Pb(Zn1/3Nb2/3)03-0.09PbTi03 near the ferroelectric critical endpoint

doi: 10.1080/00150193.2018.1470827(https://doi.org/10.1080/00150193.2018.1470827)

Double hysteresis loops in $0.91Pb(Zn_{1/3}Nb_{2/3})O_3$-$0.09PbTiO_3$ near the ferroelectric critical endpoint

Makoto IWATA,[1] Yasutaka KAIDEN,[1] Yoshinori TAKIKAWA,[1] and Yoshihiro ISHIBASHI[2]

[1] *Department of Physical Science and Engineering, Nagoya Institute of Technology, Nagoya 466-8555, Japan*

[2]*Department of Applied Physics, Nagoya University, Nagoya 464-8603, Japan*

Polarization-electric field hysteresis loops in $0.91Pb(Zn_{1/3}Nb_{2/3})O_3$-$0.09PbTiO_3$ have been investigated near the ferroelectric critical temperature in the bipolar field applied along the $[001]_c$ direction in the pseudo-cubic coordinate. The double hysteresis loop has been observed above the transition temperature indicating the field induced transition, and the ferroelectric critical endpoint has been found at 192ºC and 1.6 kV/cm. The temperature field phase diagram under the electric field applied along the $[001]_c$ direction has been clarified.

Keywords: PZN-*x*PT, hysteresis curve, critical endpoint, field-induced phase transition, temperature field phase diagram,

1. Introduction

Perovskite-type ferroelectrics (1-*x*)$Pb(Zn_{1/3}Nb_{2/3})O_3$-*x*$PbTiO_3$ (PZN-*x*PT) are important in practical applications because of their high electromechanical coupling coefficient near the morphotropic phase boundary (MPB) located at $x = 9\%$ [1-3]. PZN-*x*PT, regarded as a relaxor ferroelectric, is known to undergo the diffuse phase transition with a broad peak of the dielectric permittivity as a function of temperature owing to heterogeneity such as polar nanoregions (PNRs), where PNRs form in the paraelectric matrix below the Burns temperature [4]. To explain physical properties in relaxors, the superparaelectric model [5] and the spherical random-bond-random-field (SRBRF) model [6], assuming the thermal fluctuation of the spontaneous polarization in PNRs, were proposed, whereas Westphal *et al*. proposed the random field model in which the static random field is assumed to induce PNRs [7]. Thus, the mechanism for appearance of relaxor properties seems to be still controversial.

Kutnjak *et al*. discovered the ferroelectric critical endpoint (CEP) on the concentration-temperature-field phase diagram in (1-*x*) $Pb(Mg_{1/3}Nb_{2/3})O_3$-*x*$PbTiO_3$ (PMN-*x*PT), which is an isomorphous compound of PZN-*x*PT of the present interest, and they claimed that the giant electromechanical response in PMN-*x*PT is consistent with the existence of CEP in addition to MPB [8]. CEP in PMN-*x*PT has been extensively investigated in details by many authors [9-14], and the understanding of CEP in PMN-*x*PT has been established.

With respect to PZN-*x*PT ($x = 8\%$), the temperature-field phase diagram has been reported by means of the neutron diffraction [15]. In a series of our studies, we have investigated the field-induced phase transition in PZN-*x*PT including CEP by measuring the permittivity under the dc biasing field [16-19], and have proposed the

temperature-concentration-field phase diagram in PZN-*x*PT mixed crystal system [20]. In ref. [20], we have claimed that the decrease of heterogeneity owing to the applied electric field may make the phase transition become sharper, since the diffuseness of the phase transition is known to come from the heterogeneity of the polarization in the sample. The temperature-field phase diagram in perovskite-type ferroelectric materials was discussed based on the Landau-Devonshire free energy [21].

On the other hand, it is well-known that the field induced transition and the ferroelectric CEP can be observed by the polarization-electric field (p-E) hysteresis loop with the Sawyer-Tower circuit. However, the double hysteresis loop due to the field-induced transition in PZN-*x*PT has not been reported yet, as far as the authors know. Under this circumstance, in the present study, to reinforce our previous conclusion that the CEP certainly exists, we have observed the double hysteresis loop in PZN-9%PT showing the field induced transition above the first-order transition temperature.

2. Experimental

Single crystals of PZN-9%PT used in our experiments were acquired from Microfine materials technologies in Singapore. The typical size in platelike samples perpendicular to the $[001]_c$ direction is $3\times3\times0.2$ mm^3, where the subscript c in $[001]_c$ indicates the pseudo-cubic coordinate.

For the measurement of the dielectric permittivity, the sample plates with Au electrodes deposited on their faces were prepared. Measurements of the permittivity in the dc biasing field were carried out using an impedance/gain phase analyser (NF ZGA5900) and a high-voltage amplifier (Trek 609E-6) used as a high-voltage source.

In our measurement system, an ac probe voltage to measure the dielectric permittivity is about 100 mV, and the maximum value of the dc biasing voltage to the sample during the measurement is 800V. Complex dielectric permittivities, ε' and ε", were obtained at 41 frequencies in the range from 100 Hz to 1 MHz after carefully removing the effects of the stray capacitance and residual impedance in the system [22].

3. Results and Discussions

Figures 1(a)-(c) show temperature dependences of the dielectric permittivities under the dc biasing field of 0, 1.6, and 2.0 kV/cm along the $[001]_c$ direction in PZN-9%PT measured on heating, respectively. The frequencies of the ac probe field are 0.1, 1, 10, and 100 kHz. It is seen that almost no dielectric dispersion appears in those measurement frequencies. The broad peak at 189 ^{o}C under no field in Fig. 1(a) changes to the sharp phase transition with approaching E = 1.6 kV/cm shown in Fig. 1(b), and above this field, a broad peak appears again (see Fig. 1(c)). This indicates that CEP exists in the vicinity of E =1.6 kV/cm. In our experiment, we have confirmed that no thermal hysteresis of the dielectric permittivity appears near the CEP within experimental error.

Figures 2(a)-(d) demonstrate the p-E hysteresis loops at 200, 192, 187, and 170^{o}C, respectively. The measurement frequency is 6 Hz. As temperature decreases from 200^{o}C (Fig. 2(a)), nonlinearity in the closed p-E loop increases, and the ferroelectric CEP appears at 192 ^{o}C (Fig. 2(b)). Below the critical temperature, the closed p-E loop changes into the double hysteresis loop as shown in Fig. 2 (b), indicating the field induced transition. In the ferroelectric phase, the normal (single) hysteresis loop

showing the polarization reversal appears as shown in Fig. 2(d). Based on our result of the p-E loop observation, the critical temperature and critical field are determined to be 192ºC and 1.6 kV/cm, respectively. The detailed discussion of the p-E loop near the transition temperature was reported on the basis of the Landau-type free energy [23].

Figure 3 shows temperature-field phase diagrams with the electric field applied along the $[001]_c$ direction in PZN-9%PT. Transition points determined from p-E hysteresis loops are shown by open squares, and those determined from the temperature dependences of the permittivities under the dc biasing fields are shown by open circles. The line is the eye-guide for the cubic-tetragonal phase boundaries. The characters C and T show the cubic and tetragonal symmetries, respectively. The characters in the parentheses indicate the rigorous symmetry of the system, including the one of the electric field. The critical endpoint determined in our experiment is 192ºC and 1.6 kV/cm, and is shown with the solid circle. This indicates that CEP determined from both methods is consistent.

On the other hand, it is seen in Fig. 3 that only the phase transition temperature in the zero biasing field deviates markedly on the temperature-field phase diagram, while PZN-9%PT behaves as a normal ferroelectric material under the biasing field above about $E = 0.28$ kV/cm. This indicates that the biasing field decreases the effect of the heterogeneity of the polarization such as PNRs. The relaxor property may remain in the small field range below about $E = 0.28$ kV/cm in PZN-9%PT, because the heterogeneity cannot be completely suppressed.

4. Conclusion

In the present study, temperature dependences of the permittivity under dc field and p-E hysteresis loops in PZN-9%PT have been investigated in the field applied along the $[001]_c$ direction. The double hysteresis curve has been observed above the transition temperature indicating the field-induced phase transition. The temperature field phase diagram under the electric field applied along the $[001]_c$ direction has been clarified. CEP has been found at T_{CEP} =192ºC and E_{CEP} =1.6 kV/cm. We conclude that the relaxor property in PZN-9%PT is almost all suppressed in the dc field range above about E = 0.28 kV/cm.

Acknowledgments

This work was supported in part by JSPS KAKENHI Grant Numbers JP16K13820 to MI.

References

1. Kuwata J, Uchino K, and Nomura S: Dielectric and Piezoelectric Properties of $0.91Pb(Zn_{1/3}Nb_{2/3})O_3$-$0.09PbTiO_3$ Single Crystals. Jpn. J. Appl. Phys. 1982; **21**: 1298-1302.
2. Park S-E and Shrout TR: Ultrahigh strain and piezoelectric behavior in relaxor based ferroelectric single crystals. J. Appl. Phys. 1997; **82**: 1804-1811.
3. Samara GA: *Solid State Physics*, vol. 56: Ehrenreich H, Spaepen F, eds. Advances in Research and Applications. New York: Academic Press; 2001: 239-458.

4. Burns G and Dacol FH: Glassy Polarization Behavior in Ferroelectric Compounds $Pb(Mg_{1/3}Nb_{2/3})O_3$ and $Pb(Zn_{1/3}Nb_{2/3})O_3$. Solid State Commun. 1983; 48: 853-856.

5. Cross LE: Relaxor ferroelectrics. Ferroelectrics 1987; 76: 241-267.

6. Pirc R and Blinc R: Spherical random-bond–random-field model of relaxor ferroelectrics. Phys. Rev. B 1999; 60: 13470-13478.

7. Westphal V, Kleemann W, and Glinchuk MD: Diffuse Phase Transitions and Random-Field-Induced Domain States of the "Relaxor" Ferroelectric $PbMg_{1/3}Nb_{2/3}O_3$. Phys. Rev. Lett. 1992; 68: 847-580.

8. Kutnjak Z, Petzelt, and Blinc R: The giant electromechanical response in ferroelectric relaxors as a critical phenomenon. Nature 2006; 441: 956-959.

9. Raevskaya SI, Emelyanov AS, Savenko FI, Panchelyuga MS, Raevski IP, Prosandeev SA, Colla EV, Chen H, Lu SG, Blinc R, Kutnjak Z, Gemeiner P, Dkhil B, and Kamzina LS: Quasivertical line in the phase diagram of single crystals of $PbMg_{1/3}Nb_{2/3}O_3$-$x$$PbTiO_3$ (x =0.00, 0.06, 0.13, and 0.24) with a giant piezoelectric effect. Phys. Rev. B 2007; 76: 060101(R).

10. Vugmeister BE and Rabitz H: Kinetics of electric-field-induced ferroelectric phase transitions in relaxor ferroelectrics. Phys. Rev. B 2001; 65: 024111/1-4.

11. Dkhil B and Kiat JM: Electric-field-induced polarization in the ergodic and nonergodic states of $PbMg_{1/3}Nb_{2/3}O_3$ relaxor. J. Appl. Phys. 2001; **90**: 4676-4681.

12. Kutnjak Z, Blinc R, and Ishibashi Y: Electric field induced critical points and polarization rotations in relaxor ferroelectrics. Phys. Rev. B 2007; 76: 104102/1-8.

13. Iwata M and Yokoi R, Sugiyama Y, Maeda M, Tachi Y, and Ishibashi Y: Temperature-Field Phase Diagrams in $Pb(Mg_{1/3}Nb_{2/3})O_3$-29.5%$PbTiO_3$. Ferroelectrics 2014; 462:19-27.

14. Dul'kin E, Mojaev E, Roth M, Raevski IP, and Prosandeev SA: Nature of thermally stimulated acoustic emission from $PbMg_{1/3}Nb_{2/3}O_3$–$PbTiO_3$ solid solutions. Appl. Phys. Lett. 2009; 94: 252904/1-3.

15. Ohwada K, Hirota K, Rehrig PW, Fujii Y, Shirane G. Neutron diffraction study of field-cooling effects on the relaxor ferroelectric $Pb[(Zn_{1/3}Nb_{2/3})_{0.92}Ti_{0.08}]O_3$. Phys. Rev. B 2003; **67**: 094111.

16. Iwata M, Iijima N, Maeda M, and Ishibashi Y: Temperature–field phase diagrams in $Pb(Zn_{1/3}Nb_{2/3})O_3$–4.5%$PbTiO_3$ II. Ceramics International 2013; 39: S75-S79.

17. Iwata M, Tanaka K, Maeda M, and Ishibashi Y: Detailed Investigation of Temperature-Field Phase Diagrams in $Pb(Zn_{1/3}Nb_{2/3})O_3$–9%$PbTiO_3$. Ferroelectrics 2012; 440: 67-74.

18. Iwata M, Iijima N, and Ishibashi Y: Temperature-Field Phase Diagrams in $Pb(Zn_{1/3}Nb_{2/3})O_3$-4.5%$PbTiO_3$. Ferroelectrics 2012; 428: 1-7.

19. Iwata M, Iijima N, and Ishibashi Y: Field-Induced Phase Transition between Tetragonal and Rhombohedral Phases in $Pb(Zn_{1/3}Nb_{2/3})O_3$–8%$PbTiO_3$. Jpn. J. Appl. Phys. 2010; **49**: 09ME01/1-3.

20. Iwata M, Nagahashia R, Maeda M, and Ishibashi Y: Stable ferroelectric phases and electric field effect in a relaxor solid solution system $Pb(Zn_{1/3}Nb_{2/3})O_3$-$x$$PbTiO_3$. Phase Transitions. 2015; **88**: 306-319.

21. Iwata M, Kutnjak Z, Ishibashi Y, and Blinc R: Theoretical analysis of the temperature-field phase diagrams of perovskite-type ferroelectrics. J. Phys. Soc. Jpn. 2008; 77: 034703/1-3.

22. Iwata M, Tanaka K, Maeda M, and Ishibashi Y: Dielectric tunability near critical endpoint in $Pb(Zn_{1/3}Nb_{2/3})O_3$–$PbTiO_3$. Jpn. J. Appl. Phys. 2014; 53: 038004/1-3.

23. Iwata M and Ishibashi Y: Phenomenological Theory in Dielectric Tunable Materials with the Tristable States. Ferroelectrics 2016; 503: 7-14.

Figure captions

Fig. 1. Temperature dependences of dielectric permittivities on heating under dc biasing fields applid along the $[001]_c$ direction in PZN-9%PT, where frequencies are 0.1, 1, 10, and 100 kHz. The dc biasing fields *E* are (a) 0, (b) 1.6, and (c) 2.0 kV/cm.

Fig. 2. P-E hysteresis loops under electric fields applied along $[001]_c$ direction in PZN-9%PT, where frequency of the elelctric field is 6 Hz. Temperatures *T* are (a) 200, (b) 192, (c) 187, and (d) 170ºC.

Fig. 3. Temperature-field phase diagram with electric field applied along $[001]_c$ direction in PZN-9%PT. Transition points determined from p-E hystetresis loops are shown by open squares, and those determined from temperature dependence of the permittivities under dc biasing fields are shown by solid circles. Line is eye-guide for the concerned phase boundary. Characters C and T show the cubic and tetragonal symmetries, respectively. Characters in the parentheses indicate the rigorous symmetry under the electric field along the $[001]_c$ direction.

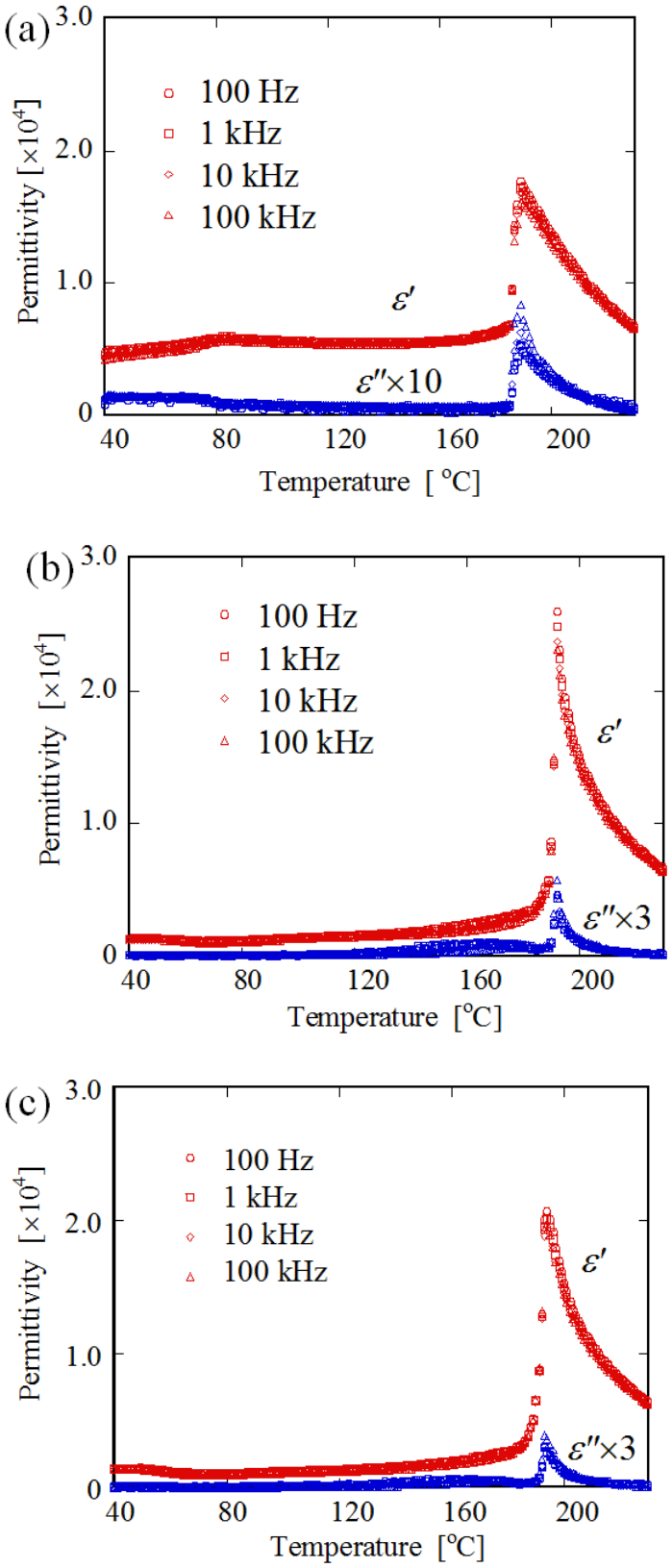

Fig. 1. Temperature dependences of dielectric permittivities on heating under

dc biasing fields applid along the $[001]_c$ direction in PZN-9%PT, where frequencies are 0.1, 1, 10, and 100 kHz. The dc biasing fields E are (a) 0, (b) 1.6, and (c) 2.0 kV/cm.

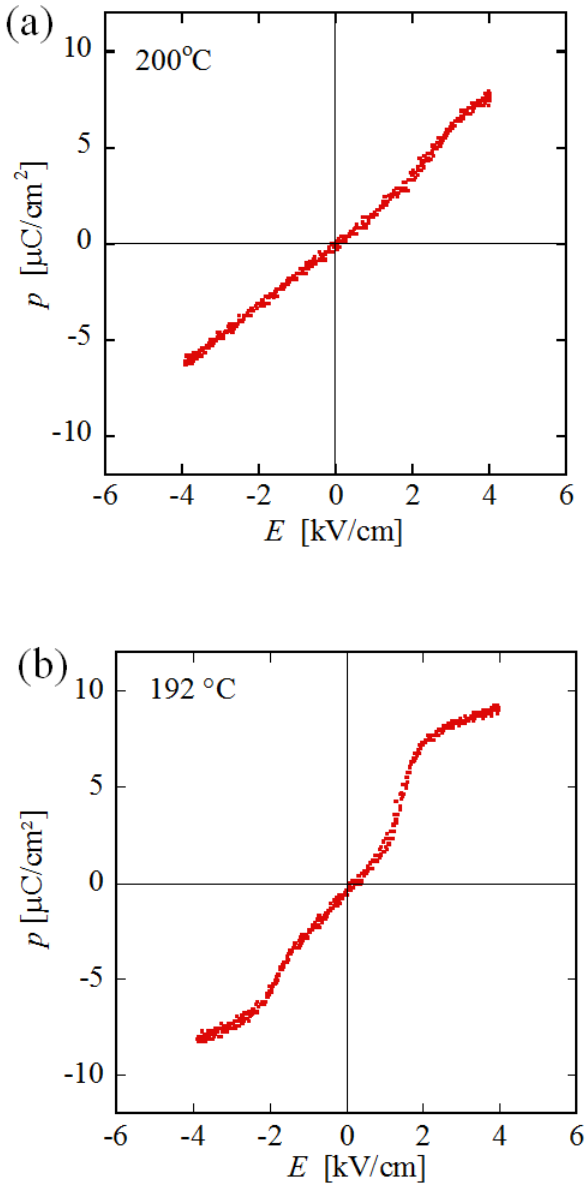

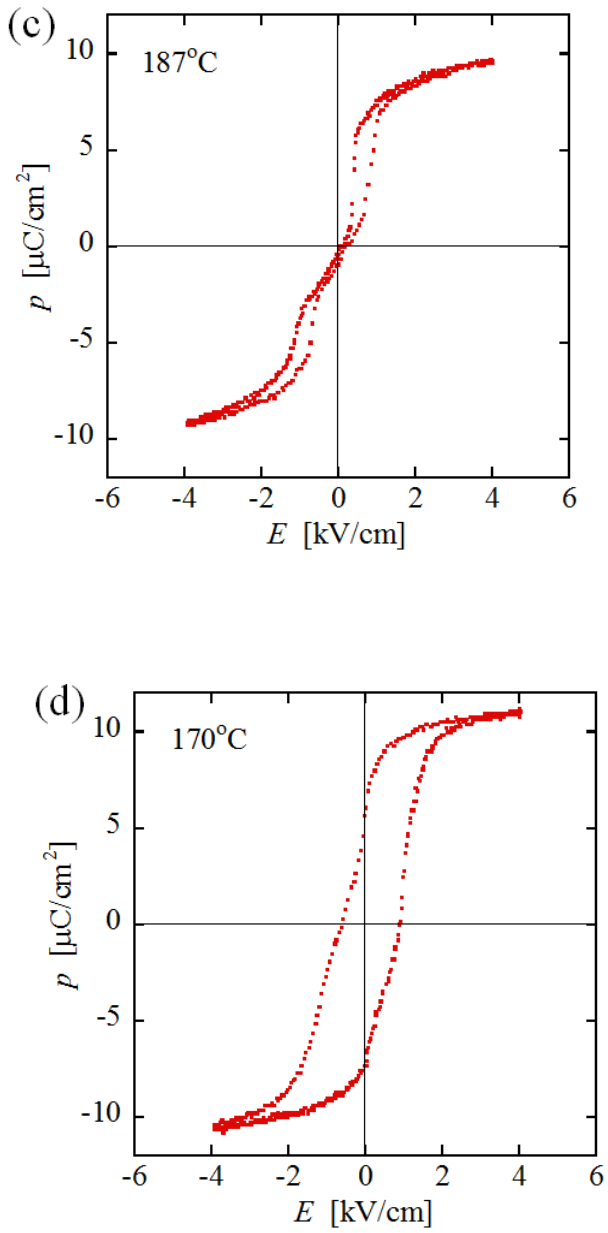

Fig. 2. P-E hysteresis loops under electric fields applied along $[001]_c$ direction in PZN-9%PT, where frequency of the elelctric field is 6 Hz. Temperatures T are (a) 200, (b) 192, (c) 187, and (d) 170°C.

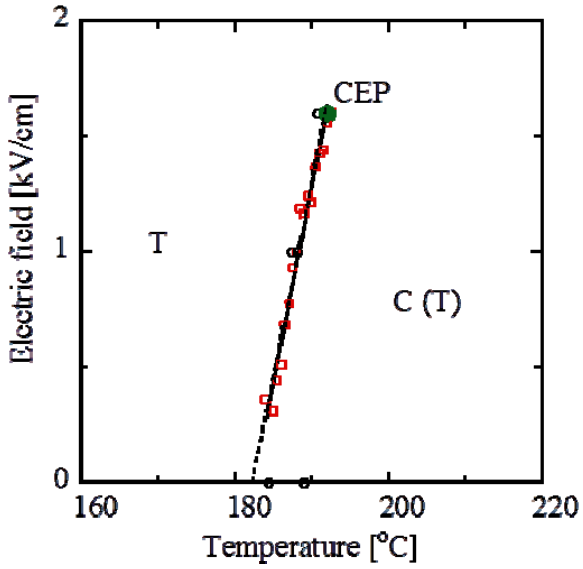

Fig. 3. Temperature-field phase diagram with electric field applied along $[001]_c$ direction in PZN-9%PT. Transition points determined from p-E hystetresis loops are shown by open squares, and those determined from temperature dependence of the permittivities under dc biasing fields are shown by open circles. Line is eye-guide for the concerned phase boundary. Characters C and T show the cubic and tetragonal symmetries, respectively. Characters in the parentheses indicate the rigorous symmetry under the electric field along the $[001]_c$ direction.